Self-consistent embedded-cluster model for magnetic impurities: Fe, Co, and Ni in β'-NiAl

D. E. Ellis, G. A. Benesh, and E. Byrom*

*Department of Physics and Astronomy and Materials Research Center,
Northwestern University, Evanston, Illinois 60201*

(Received 24 April 1978; revised manuscript received 20 April 1979)

Substitutional transition-metal impurities occupying either Ni or Al sites in the intermetallic compound β'-NiAl with CsCl structure have been treated by a self-consistent molecular-orbital method. The electronic energy levels and charge and spin densities of MX_8 clusters representing a central atom and its nearest neighbors and MX_8Y_6 clusters representing central, nearest-neighbor and second-nearest-neighbor atoms have been calculated in the Hartree-Fock-Slater spin-polarized model, using a numerical discrete variational method. Interaction of the impurity cluster with the crystal environment is represented by a pseudopotential derived from cluster calculations on the pure compound. Results for Fe, Ni, and Co impurities in β'-NiAl are discussed in connection with experimental resistivity, Mössbauer isomer shift, and NMR data.

I. INTRODUCTION

NiAl, an ordered stoichiometric alloy of nickel and aluminum, crystallizes in the β' phase, $B2$ structure of which CsCl is the prototype. In the absence of magnetic impurities, the alloy is a Pauli paramagnet.[1,2] However, when these impurities are introduced, several low-temperature anomalies appear in the magnetic and transport properties. These anomalies include a Curie-law susceptibility,[2,3] a minimum in the resistivity versus temperature curve,[4-7] a negative magnetoresistance,[5,6,8] and the deviation of the ^{27}Al NMR relaxation time T_1 from the reciprocal temperature dependence of pure β'-NiAl samples.[9] Our work is especially motivated by detailed investigations of the dependence of the magnetic properties on composition: Ni_xAl_{1-x}, Fe-doped Ni_xAl_{1-x}, and $(NiAl)_{1-x}M_x$ where M is a $3d$ transition metal, for various values of x.[6,7,10]

These effects are characteristic of those caused by similar impurities in simple metals such as Al, Cu, and Au which have s-like conduction bands and are also Pauli paramagnetic. The electronic structure of magnetic impurities in host metals has been probed by many techniques, including low-temperature resistivity measurements, NMR, Mössbauer nuclear γ-ray resonance, magnetic susceptibility χ, and neutron scattering. Results from these experiments have led to theories based on the scattering of Bloch waves from the impurity potential. A scattering resonance corresponding to the impurity d state is formed, and the relative magnitudes of the Coulomb repulsion between d electrons at the impurity, and the width of the resonance, determine whether or not a magnetic

moment is formed at the impurity. All of these factors depend primarily upon the immediate environment of the impurity atom, suggesting that finite-cluster models can account for many of the observed properties.

Binary alloys like β'-NiAl, in which the magnetic TM atoms interact weakly provide a suitable medium for developing local cluster models. We have performed first-principles calculations on small clusters to elucidate details of the bonding interactions which determine localized charge and spin densities. A further goal of the present work is to determine whether such cluster models based predominantly on nearest-neighbor interactions are able to predict the presence or absence of a moment, and to obtain estimates of the relative magnitude of the cluster moments and their spatial distribution. We have thus utilized the spin-unrestricted self-consistent Hartree–Fock–Slater (HFS) molecular-orbital method[11] to study a number of MX_8 and MX_8Y_6 model systems appropriate to transition-metal impurities in β'NiAl.

II. THEORETICAL MODEL AND COMPUTATIONAL PROCEDURE

A. Hartree-Fock-Slater model

In this paper all calculations were performed using the HFS local-density one-electron model. In this model, the Hamiltonian consists of the sum of a kinetic energy operator, nuclear and electron Coulomb potentials, and an exchange potential. The essential point of this theory is that the nonlocal ex-

1198

change operator of the Hartree—Fock theory is ap-
proximated by a local exchange potential. In the
spin-polarized formalism, this potential is given (in
Hartree a.u.) as

$$V_{ex,\sigma} = -3\alpha \left[\frac{3\rho_\sigma(\vec{r})}{4\pi} \right]^{1/3} , \qquad (1)$$

where ρ_σ is the density of electrons of spin σ. The
Kohn—Sham value of the exchange scaling parame-
ter, $\alpha = \frac{2}{3}$, can be compared to the "full Slater" value
of one, and the so-called $X\alpha$ values which are inter-
mediate to the above.[12] The value $\alpha = \frac{2}{3}$ is common-
ly used in self-consistent energy-band models,[13] and
it is understood that slightly larger values simulate
some part of the correlation potential in addition to
exchange. We have used the value $\alpha = 0.70$
throughout the present work, guided by a variety of
molecular studies. Recently, various authors have
derived local potentials representing both exchange
and correlation which are, in principle, better justified
than that in Eq. (1).[14] However, differences between
these potentials are too small to be of any importance
here.

b. Energy band versus molecular cluster approach

The HFS model has been successfully applied to a
variety of metallic systems using both periodic Bloch
functions and localized molecular clusters. In partic-
ular, augmented plane wave (APW) band-structure
calculations of Connolly and Johnson for β'-NiAl
have been compared with optical data.[15] Moruzzi
et al.[16] have presented self-consistent Korringa-
Kohn-Rostoker (KKR) results for this system in or-
der to discuss d band narrowing in transition-metal
alloys. The general agreement between the two
band-theory models and features of optical and ultra-
violet photoemission spectroscopy (UPS) data is quite
satisfactory. We shall discuss the band calculations
further in connection with the photoelectron data and
the cluster results.

Approximate treatment of isolated impurities in a
metal by band theory is also possible, making use of
the so-called super-cell method. Here one considers
a large unit cell containing the impurity atom and a
sufficient number of host atoms to (hopefully)
reduce the interaction between the periodic array of
impurities to a negligible level. In practice, such cal-
culations are very tedious and have been carried out
in only a few cases.[17] The Green's function formal-
ism allows a rigorous self-consistent treatment of
impurity-host interactions, but nonempirical calcula-
tions require explicit manipulation of Bloch wave
functions for the unperturbed solid. Successful appli-
cations have been made to simple systems, e.g., the

idealized defect (vacancy) in silicon.[18] Such calcula-
tions are again very tedious.

Molecular cluster models offer the possibility of
treating localized impurity or defect structures in
solids with minimal computational effort. Numerous
HFS metal cluster studies have been made which il-
lustrate the utility of this approach in interpreting
metal-metal bonding, photoelectron spectra, chem-
isorption properties, etc.[19-24] The problem of conver-
gence to the infinite solid can be treated either by
taking larger and larger clusters, or by developing
suitable boundary conditions for small clusters. We
believe that the latter approach is ultimately more
fruitful, in placing emphasis on localized interactions
in the presence of the extended crystalline environ-
ment. We have previously reported on the use of
simplified embedding models for LiAl[25] and have
given a brief discussion of magnetic impurities in β'-
NiAl.[26]

C. Variational method

Numerical free-atom basis functions $\{A_j\}$ were
used to obtain the molecular eigenfunctions as a
linear combination of atomic orbitals (LCAO),

$$\psi_i(r) = \sum_j A_j(r) C_{ji} . \qquad (2)$$

We have obtained these basis functions by numeri-
cally solving the Schrödinger equation for a discrete
set of sample points. Two independent sets of basis
functions were used in these calculations: one in
which a spherical well of depth 4 a.u. and radius 6
a.u. was added to each atomic potential prior to solv-
ing the Schrödinger equation, and one in which no
well was added. In both bases $4s$ and $4p$ states are
included on the transition-metal atoms. The well was
added in one basis set in order to limit the radial ex-
tent of the more diffuse orbitals, thus reducing the
overlap between atomic orbitals centered on different
atoms and obtaining a somewhat better variational
basis. Core levels are therefore not affected.

The discrete variational method (DVM) used is
described elsewhere in the literatue.[27] Briefly, energy
eigenvalues and eigenvector coefficients C_{ji} are deter-
mined by solving a secular equation obtained by
minimizing an error functional. Matrix elements of
the Hamiltonian and unit (overlap) operators were
calculated by three-dimensional numerical integra-
tion. A numerical precision of ~ 0.3 eV in valence
level energies was obtained with 1500 integration
points.

D. Crystal potential

One may expect that the external boundary condi-
tions imposed on a cluster model will have highly sig-
nificant effects because of the diffuse nature of me-

tallic wave functions. Thus point-charge or boundary-sphere approximations commonly used in cluster calculations on ionic and covalent solids will be inadequate. We have chosen to construct a crystal potential for bulk β'-NiAl from the cluster self-consistent charge density ρ_{scc}. The main point of this procedure is the approximate decomposition of the cluster density by Mulliken populations, as

$$\rho_{\text{cluster}} \approx \rho_{\text{scc}} = \sum_{\nu nl} f_{nl}^{\nu} |R_{nl}(r_{\nu})|^2 \ , \tag{3}$$

where f_{nl}^{ν} is the population for atom ν of the nl atomic shell as determined from occupied molecular eigenvectors. The crystal charge density for successive iteration cycles is then constructed by summing over all atoms, then averaging results from previous cycles in the usual fashion [see Fig. 1(a)].

For the case of dilute TM impurities in β'-NiAl, we chose to embed the clusters in the self-consistent crystal field that had been calculated for bulk β'-NiAl. Thus, the effects of the TM impurity were restricted to the nearest-neighbor environment in the MX_8 clusters and the second neighbors in MX_8Y_6 clusters. This model is probably adequate for dilute magnetic systems as in the present case, but clearly inadequate for systems like MnPd, for which the polarization extends over many shells of neighbors. Cohen and
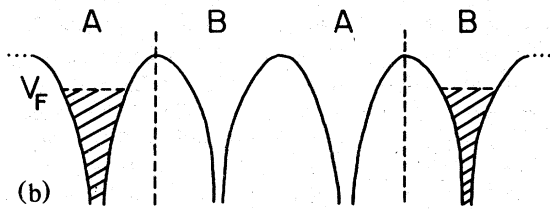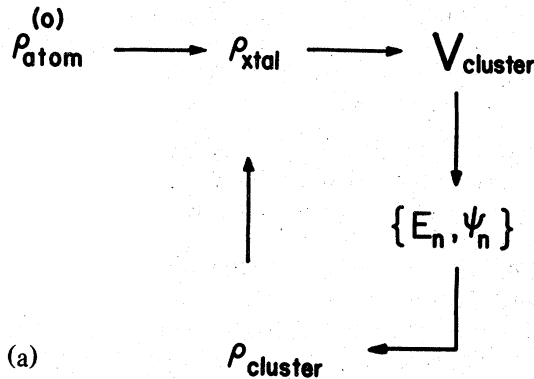

FIG. 1. (a) Schematic of self-consistency loop for cluster embedded in the solid. (b) Schematic of truncated crystal potential used in calculating AB cluster levels embedded in the periodic solid.

Slichter have presented a semiempirical one-electron model in which the magnetic ion interacts with a homogenous medium, and applied this model to TM impurities in copper.[28] We suggest that a similar approach, based upon an AB_{12} cluster embedded in the polarized medium, could describe both local bonding and long-range polarization effects.

As described elsewhere,[25] a one-parameter pseudo-potential in which potential wells localized on atoms exterior to the cluster are truncated at an energy V_F is employed to stabilize charge transfer between the cluster and crystal [see Fig. 1(b)]. This potential simulates effects of the Pauli exclusion principle by preventing cluster electrons from populating occupied states localized on exterior wells in the crystal. Variation of properties with this potential floor V_F has been found to be slight. There is some virtue in choosing $V_F = E_F$, i.e., at the Fermi level, but values in the range of 5–10 eV produce very acceptable results.

Since the clusters studied here are non-stoichiometric, charge transfer produces some small electron flow to or from the cluster. We have chosen to renormalize valence occupation numbers to guarantee a neutral unit cell. This has been found to be a satisfactory procedure which also allows us to reconcile slight differences found between Ni-centered and Al-centered clusters.[25,26] The bulk calculations were used to determine the ionicity of the atoms in the crystal potential, and to estimate the total charge (q) on the cluster itself. For all of the clusters used, we have found $|q| \le 1$, and that the ionicity of each atom is relatively small. It would be desirable to use a stoichiometric NiAl cluster in which q is obviously zero; however, these clusters are all of lower than cubic symmetry. We have preferred to use clusters exhibiting the full O_h point-group symmetry of the alloy itself, for reasons of computational efficiency.

E. Density of states

The energy spectrum of valence eigenfunctions is best displayed as an energy density of states (DOS). The sharp details of the DOS due to the finite-cluster levels are not relevant to our approximate description of the bulk crystal, so a smoothed version was adopted. The contribution of state nl of atom ν to the DOS is represented by

$$D_{nl}^{\nu}(E) = \sum_p f_{nl,p}^{\nu} \frac{\sigma/\pi}{(E - \epsilon_p)^2 + \sigma^2} \ , \tag{4}$$

where $f_{nl,p}^{\nu}$ is the appropriate Mulliken population[29] contribution to the pth molecular orbital. The Lorentzian width parameter σ was chosen to be 1 eV, a value consistent with the uncertainties of our

calculations and the small cluster size. By summing over all partial DOS, we obtain the total DOS

$$D(E) = \sum_{vnl} D_{nl}^{v} = \sum_{p} \frac{\sigma/\pi}{(E - \epsilon_p)^2 + \sigma^2} \quad . \qquad (5)$$

III. RESULTS

A. Bulk NiAl properties

To gain an impression of the deviations between cluster densities of states and full band-structure results, and to determine the self-consistent atomic configurations of the cluster and crystal atoms, we performed our first calculations on two molecular clusters exhibiting the full O_h point-group symmetry of β'-NiAl. Each cluster consisted of a central atom, either Ni or Al, and its eight nearest neighbors (Al or Ni). The cube edge was taken as 5.442 a.u.[30]

As previously described, the cluster potential was constructed from a self-consistent embedding model based upon the Mulliken population analysis. Inclusion of Coulomb and exchange interaction with the atoms external to the cluster proved essential in obtaining charge densities and densities of states which were relatively invariant to the cluster origin (AlNi$_8$ or NiAl$_8$) and to atom position (center versus periphery of cluster). In discussing atomic populations, such as Ni $3d$, within the cluster itself, we have used the Mulliken population analysis outlined in Sec. II D, to approximately decompose cluster states. This analysis is useful for qualitative and some semiquantitative interpretations of orbitals that are localized on specific atoms; however it can be misleading when used on diffuse, strongly overlapping basis functions such as transition-metal $4p$ states. As an example, we calculated a "Mulliken radius" for the central Ni atom in a NiAl$_8$ cluster by integrating the charge density out to a radius at which the total charge matched that obtained from the Mulliken analysis. This radius of 2.85 a.u. exceeds both the Wigner–Seitz radius (2.68 a.u.) and one-half of the Ni-Al bond distance (2.36 a.u.). Thus the Mulliken populations here describe some extremely diffuse electron charge that is actually closer to neighboring Al atoms.

The partial density of states analysis gives the Ni $3d$ and Al $3s + 3p$ curves shown at the bottom of Fig. 2. The total band DOS found by Connolly and Johnson[15] using a non-self-consistent APW method is reproduced for comparison in Fig. 2, top. The self-consistent KKR results of Moruzzi et al. are quite similar.[16] We have also included the XPS data of Kowalczyk et al.[31] In the figure we have chosen to align the large, central peak common to three of the curves. These data are consistent with the general analysis of UPS data given by Nilsson[32] and reveal
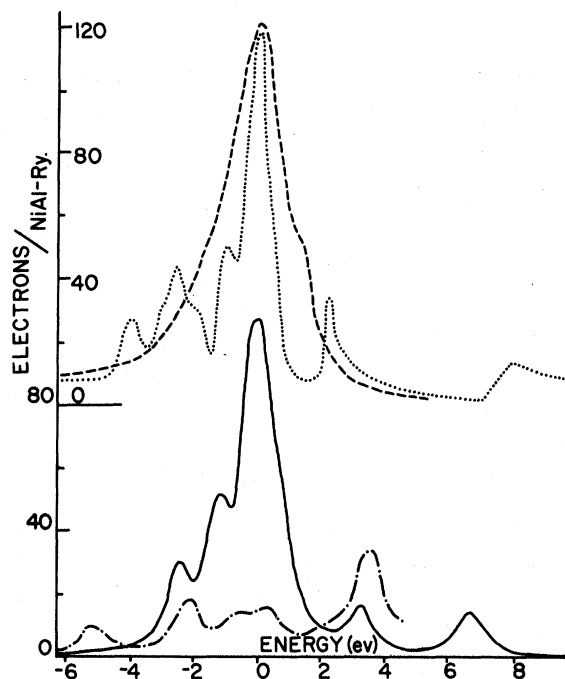

FIG. 2. Top: Total band DOS as calculated by Connolly and Johnson (dotted line) and XPS results of Kowalczyk et al. (dashed line). The prominent $3d$ peak in the DOS has been aligned with the XPS peak. Bottom: Partial density of states for Ni $3d$ character (solid line) and Al $3s + 3p$ character (broken line) from NiAl$_8$ and AlNi$_8$ clusters.

further details of interest. Our partial DOS results show that the prominent peak in the band DOS consists primarily of Ni $3d$ character, and that the small peak at about 3 eV on the figure is composed of Ni $3d$, Al $3s$, Al $3p$, and Ni $4s$ states. Although the cluster DOS is *not* an accurate representation of the complete energy band DOS of the periodic solid, we find the overall comparison quite satisfactory.

To give some idea of the variability of predictions of atomic configurations which would be found from iterating different clusters, we present some representative data in Table I. Here we have taken three crystal potentials: (i) the "self-consistent configuration" obtained by averaging the results of the NiAl$_8$ and AlNi$_8$ clusters described above; (ii) a neutral atom superposition; and (iii) our estimate of an "ionic extreme". These three potentials are designated as Ni$^{-0.12}$Al$^{+0.12}$, Ni^{0}Al^0, and Ni$^{-0.59}$Al$^{+0.59}$, respectively. We have also included in this table results for the minimal NiAl$_8$ and AlNi$_8$, as well as NiAl$_8$Ni$_6$ and AlNi$_8$Al$_6$ clusters in which the next-nearest-neighbor atoms have been added to the minimal clusters. For greater variational freedom, we have allowed the central and peripheral atoms to vary independently. The entry labeled Ni$_7$Al$_8$ represents a NiAl$_8$Ni$_6$ cluster in

TABLE I. Self-consistent atomic charges for clusters embedded in different crystal potentials.

Cluster	Basis set[a]	Crystal potential	Al Ion	Ni Ion
$NiAl_8$	1	$Ni^{-0.12}Al^{+0.12}$	+0.12	−0.08
$NiAl_8$	2	$Ni^{-0.12}Al^{+0.12}$	+0.12	−0.11
$AlNi_8$	2	$Ni^{-0.12}Al^{+0.12}$	+0.25	−0.14
$NiAl_8Ni_6$	2	$Ni^{-0.12}Al^{+0.12}$	+0.14	$−0.14^b, −0.15^c$
$AlNi_8Al_6$	2	$Ni^{-0.12}Al^{+0.12}$	$+0.30^b, +0.20^c$	−0.20
Ni_7Al_8	2	$Ni^{-0.12}Al^{+0.12}$	+0.16	−0.17
$NiAl_8$	2	Ni^0Al^0	+0.04	−0.29
$NiAl_8Ni_6$	2	Ni^0Al^0	−0.00	$−0.06^b, +0.02^c$
$NiAl_8$	2	$Ni^{-0.59}Al^{+0.59}$	+0.50	+0.16
$NiAl_8Ni_6$	2	$Ni^{-0.59}Al^{+0.59}$	+0.54	$−0.53^b, −0.54^c$

[a]Basis set 1 is for free atoms: Ni $1s \cdots 3d, 4s, 4p$ Al $1s \cdots 3s, 3p$. Basis set 2 is for atoms embedded in a potential of radius 6 a.u. and depth 4 a.u.
[b]Peripheral atom.
[c]Central atom.

which the central and peripheral Ni's are averaged together in each cycle. We have preferred the basis set labeled 2 in which wells of radius 6 a.u. and depth 4 a.u. have been added to the atomic potentials.

As Table I shows, these data indicate that of the three potentials used, the $Ni^{-0.12}Al^{+0.12}$ configuration gives most consistent results of the same sign and approximate size for all cluster types. The other two potentials induce electron configurations that vary in both sign and magnitude among the different clusters. On the basis of the apparent stability of all cluster types in the "self-consistent" crystal potential $Ni^{-0.12}Al^{+0.12}$, we decided to treat the embedded TM impurity clusters in this environment. Further iteration of the self-consistent loop would probably produce a slight increase in ionicity.

B. Transition-metal impurities

The addition of a small amount of certain transition-metal impurities to bulk NiAl causes several low-temperature magnetic and transport anomalies. These anomalies were originally thought to be intrinsic to β'-NiAl. The existence of such phenomena as negative magnetoresistance and a resistivity minimum led Yamaguchi and Brittain[8] to discuss the possibility of localized magnetic moments and the applicability of Kondo's dilute-alloy theory.[33] However, it seemed unlikely that clustered Ni atoms were the source of local moments since the magnitude of the negative magnetoresistance was found to *decrease* with increasing Ni concentration. Caskey, Franz, and Sellmyer observed that the occurrence of a Curie-like contribution to the magnetic susceptibility, resistance minima and maxima, and the negative

magnetoresistance could be attributed to the presence of localized magnetic moments.[5] Three possible causes of the moments were proposed: (i) an intrinsic band-structure effect; (ii) an impurity effect; and (iii) a defect structure associated with clusters of Ni atoms. They concluded that none of these possibilities was completely self-sufficient. The impurity atom explanation was rejected because it was inconsistent with the reported Curie susceptibility and the existence of resistance minima for Ni concentrations of less than 50%. (The latter would force TM impurity atoms onto nonmagnetic Ni sites).

Later, Willhite et al. published studies of the magnetic susceptibility, resistivity, magnetoresistance, and NMR properties of very pure NiAl samples.[1] In contrast to the earlier reports they found a positive, nearly temperature-independent magnetoresistance, a temperature-independent ^{27}Al Knight shift, and the absence of either a Curie term in the susceptibility or the occurrence of resistivity minima. They concluded that the "Kondo-like anomalies" previously observed were due to contamination of the samples with magnetic impurities, probably Fe.

Since 1973 several other experimental papers have supported the conclusions of Willhite and collaborators. Of particular interest are the resistivity measurements of Yoshitomi, Ochiai, and Brittain,[6,10] and Ochiai and Brittain.[7] While their studies of pure, near stoichiometric NiAl showed no resistance minima or maxima, similar studies of $(NiAl)_{1-x}M_x$ revealed the existence of these minima for $M = Cr$, Mn, Fe, and the absence of the minima for $M = Ti$, V, Co. Finally, a report of Fe-doped Ni_xAl_{100-x} indicates that there is no resistivity minimum for concentrations $x < 49.5$. This latter result conflicts with an earlier measurement of Yamaguchi et al.[4]

We have previously outlined theoretical models which can be used to describe magnetic impurity phenomena; here we discuss the application of cluster techniques to this problem. In this section we address several questions that the experimental results have raised: (i) Can spin-polarized cluster calculations for a TM atom surrounded by eight nearest-neighbor Ni atoms predict the presence or absence of magnetic moments in NiAl? Can these same calculations predict the presence or absence of a moment when a TM atom is surrounded by eight nearest-neighbor Al atoms? (ii) What is the nature of the metallic bonding as a function of lattice site occupation? (iii) What effects do cluster size differences make on the calculation?

We have performed self-consistent calculations on MAl$_8$, MNi$_8$, MAl$_8$Ni$_6$, and MNi$_8$Al$_6$ clusters, for M = Fe, Co, Ni. If the presence or absence of resistivity minima indicates the formation or absence of local moments, then we expect that in the MNi$_8$ and MNi$_8$Al$_6$ environments, Fe will form a moment while Co and Ni will not. We want to know what cluster models can show about such a formation. All of the clusters were embedded in the NiAl crystal produced by the bulk calculations as described earlier. The

resulting orbital populations and spin densities are listed in Tables II and III. In addition to the spin-polarized calculations presented here, spin-restricted calculations have also been performed and are published elsewhere.[26]

Let us first examine the similarities and differences between the MX_8 cluster calculations as listed in Table II. Column a lists the total population, and column b lists the magnitude and distribution of the magnetization of each cluster. It is apparent that the MNi$_8$ clusters have larger magnetic moments than the corresponding MAl$_8$ clusters. However, we are here treating only the static limit of what may be a strongly time-dependent phenomenon. In the MNi$_8$ clusters, the eight Ni atoms contribute heavily to the total moment since all have spin densities of the same sign. In the physical crystal these atomic moments may *not* be coupled, and may therefore cancel each other on the time average. We have also included the bulk AlNi$_8$ cluster calculation in Table II. This cluster also shows a fairly large moment of $4.11\mu_B$, all of which is contributed by the Ni atoms; but the experimental results strongly suggest that a cluster of this type should be nonmagnetic. What may be required for local moments to form is a

TABLE II. Self-consistent atomic-orbital populations for MX_8 clusters embedded in β'-Ni$^{-0.12}$Al$^{+0.12}$.

Orbital	M = iron		MAl$_8$ populations cobalt		nickel	
M 3d	7.06[a]	0.17[b]	7.96[a]	0.52[b]	8.86[a]	0.30[b]
4s	0.42	0.02	0.53	0.03	0.62	0.05
4p	0.21	0.14	0.51	0.25	0.75	0.71
Net charge	+0.32	0.33	+0.00	0.80	−0.23	1.06
Al 3s	1.76	0.00	1.73	−0.01	1.76	−0.01
3p	1.18	0.17	1.17	0.23	1.11	0.18
Net charge	+0.07	0.17	+0.10	0.22	+0.13	0.17
Net spin moment		1.74		2.58		2.41

Orbital	M = iron		MNi$_8$ populations cobalt		nickel		aluminum	
M 3d	6.56[a]	0.73[b]	7.42[a]	0.49[b]	8.58[a]	0.95[b]	3s 1.36[a]	−0.07[b]
4s	0.93	0.00	0.98	0.00	0.85	0.01	3p 1.39	−1.14
4p	1.56	0.01	1.98	0.01	0.50	0.02		
Net charge	−1.02	0.74	−1.35	0.50	+0.08	0.98	+0.25	−0.21
Ni 3d	8.79	0.56	8.78	0.58	8.81	0.60	8.81	0.65
4s	0.91	0.02	0.86	0.02	1.03	−0.01	1.13	−0.06
4p	0.29	0.02	0.20	0.01	0.28	0.01	0.20	−0.05
Net charge	+0.02	0.59	+0.06	0.61	−0.12	0.60	−0.14	0.54
Net spin moment		5.46		5.38		5.78		4.11

[a]Net population, ↑ + ↓ occupation.
[b]Net spin density, ↑ − ↓ occupation.

TABLE III. Self-consistent atomic-orbital populations for MX_8Y_6 clusters embedded in β'-Ni$^{-0.12}$Al$^{+0.12}$.

Orbital	MAl_8Ni_6 populations M = iron		cobalt		nickel	
$M\,3d$	6.95[a]	1.10[b]	7.94[a]	0.93[b]	8.94[a]	0.16[b]
$4s$	0.29	0.04	0.29	0.03	0.24	0.02
$4p$	0.92	0.12	1.02	0.14	1.06	0.06
Net charge	−0.15	1.26	−0.24	1.10	−0.22	0.23
Al $3s$	1.56	0.06	1.56	0.06	1.53	0.04
$3p$	1.35	0.09	1.38	0.05	1.32	0.11
Net charge	+0.09	0.15	+0.06	0.11	+0.15	0.15
Ni $3d$	8.88	0.14	8.88	0.12	8.86	0.11
$4s$	0.94	0.05	0.90	0.06	1.08	0.02
$4p$	0.26	0.09	0.24	0.05	0.21	0.02
Net charge	−0.07	0.28	−0.03	0.23	−0.15	0.15
Net MAl_8 moment		2.46		1.98		1.43

Orbital	MNi_8Al_6 populations M = iron		cobalt		nickel		aluminum	
$M\,3d$	6.77[a]	0.72[b]	7.64[a]	0.80[b]	8.78[a]	0.32[b]	$3s$ 1.03[a]	0.00[b]
$4s$	0.65	0.02	0.60	0.02	0.56	0.02	$3p$ 1.69	0.01
$4p$	1.10	0.06	1.14	0.06	0.69	0.03		
Net charge	−0.46	0.80	−0.32	0.88	+0.02	0.37	+0.30	0.01
Ni $3d$	8.78	0.15	8.80	0.16	8.78	0.11	8.89	0.01
$4s$	0.82	0.02	0.81	0.02	0.90	0.01	0.84	0.00
$4p$	0.56	0.04	0.58	0.04	0.59	0.01	0.49	0.06
Net charge	−0.15	0.22	−0.17	0.22	−0.25	0.14	−0.20	0.07
Al $3s$	1.50	0.01	1.49	0.01	1.45	0.00	1.53	0.00
$3p$	1.27	0.03	1.28	0.03	1.26	0.00	1.28	0.08
Net charge	+0.23	0.05	+0.24	0.05	+0.30	0.00	0.20	0.08
Net MNi_8 moment		2.56		2.64		1.49		0.64

[a]Net population, ↑ + ↓ occupation.
[b]Net spin density, ↑ − ↓ occupation.

strong atomic moment on a TM impurity which couples the moments on neighboring atoms. We are reminded of theories of fluctuating spin moments which are increasingly invoked to explain properties of ferromagnets near and above the Curie temperature.[34] The AlNi$_8$ cluster does not possess a strong, central moment and the MAl$_8$ clusters do not possess sizable moments on the nearest neighbors.

There is a striking difference in the magnetization density of FeNi$_8$ versus FeAl$_8$ as Fig. 3 shows. The size of the cluster moments are 5.46 and 1.74μ_B, respectively. In FeAl$_8$, the Fe moment is found in core and $3d$, $4p$ hybrid levels while the smaller Al $3p$ polarization is diffuse and largely off the bonding axis. However, in FeNi$_8$, a large polarization is induced in the neighboring Ni atoms causing the total moment to be shared more equally among the consti-
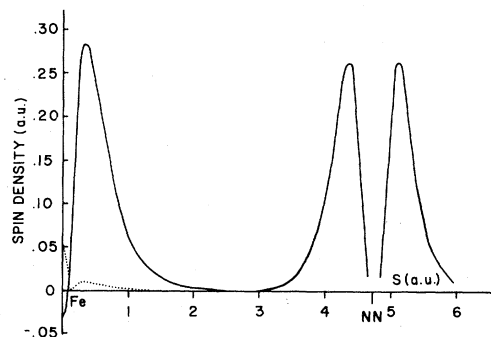

FIG. 3. Self-consistent spin density for MX_8 clusters embedded in β'-NiAl plotted along M-X bond: Fe-Ni bond in FeNi$_8$ cluster (solid line) and Fe-Al bond in FeAl$_8$ cluster (dotted line).

tuent atoms. If the experimental interpretation of Ochiai and Brittain is correct,[7] then the substitution of Fe on the Al lattice, as represented by FeNi$_8$, causes a local moment to form. This is exhibited in our present model by a sizable polarization of all cluster atoms. In contrast, a substitutional Fe atom on the Ni lattice (FeAl$_8$) induces a much smaller polarization in the neighboring atoms, which apparently time averages to zero.

It may be helpful to compare the present spin-polarized Ni$_9$ cluster results with those obtained by Messmer *et al.*[21] on Ni$_8$ and Ni$_{13}$ clusters with parameters representative of bulk nickel. Their main findings of interest here are:

(i) A reduced "d-band" width compared to bulk Ni, which increases from Ni$_8$ to Ni$_{13}$, as expected;

(ii) A self-consistent paramagnetic state, with a spin moment of $0.25\mu_B$/atom and $0.46\mu_B$/atom for Ni$_8$ and Ni$_{13}$, respectively. This result was compared favorably with observed reduced magnetization of small Ni particles and the bulk ferromagnetic moment of $0.54\mu_B$/atom.

The Ni-Ni distance in the Ni$_9$ impurity cluster of β'-NiAl, $4.71a_0$, is rather close to that of bulk Ni, and we find a paramagnetic moment of $0.64\mu_B$/atom. This value is somewhat larger than the bulk value, and is a feature which we find to be sensitive to cluster size. Thus, the NiNi$_8$Al$_6$ cluster, yields a reduced moment of $0.17\mu_B$/atom.

In Table III we present data for the MX_8Y_6 cluster calculations. The populations of the second-nearest-neighbor Al's in the MNi$_8$Al$_6$ calculations are very similar to those of the nearest-neighbor Al's in the MAl$_8$Ni$_6$ systems. These similarities lend support to our approximation of the crystal field. If the model potential were far from that actually experienced by equivalent atoms, we would expect to see Al populations differing notably between sites. We are also encouraged by similarities between the nearest-neighbor Ni's in MNi$_8$Al$_6$ clusters and the second-nearest-neighbor Ni's in MAl$_8$Ni$_6$. The significant difference between $4p$ populations, with interior atomic levels more heavily occupied, can be interpreted as formation of directed bonds toward second neighbors.

The nearest-neighbor bonds are very similar in the nine and fifteen atom clusters. Along the Fe-Ni bond in both FeNi$_8$ and FeNi$_8$Al$_6$ the charge density falls to the minimal value of $\rho = 0.045a_0^{-3}$ at $r = 2.42$ a.u. (relative to the central Fe). Similarly the minimum in the Fe-Al bond in both FeAl$_8$ and FeAl$_8$Ni$_6$ is at $r = 2.83$ a.u. and has the value $\rho = 0.040a_0^{-3}$. The charge density profile along the bond is very smooth, with no evidence of a covalent-bond "bump". However, charge is localized to the bond with angular variation of $\geq 25\%$ in ρ observed at the midbond radius.

The charge densities along the second-neighbor bond lines are also similar in both the MX_8 and

MX_8Y_6 clusters. For example, the minimum in the cluster charge density along the Fe-Al (100) line in FeNi$_8$Al$_6$ is $\rho = 0.030a_0^{-3}$ at $r = 2.83$ a.u. (the Fe-Al distance is 5.44 a.u.). The total charge density in the corresponding FeNi$_8$ cluster (found by adding the densities from exterior atoms to the cluster density) also has a minimum of $\rho = 0.033a_0^{-3}$ at this radius. In the latter case the exterior atom charge-density contribution is not negligible, and is therefore included.

The magnetization distribution of MX_8Y_6 clusters differs considerably from that of minimal clusters, with the average moment per site reduced in the larger clusters. The second-neighbor Al atomic moment is $0.1\mu_B$ less than that of the first-neighbor Al (in MAl$_8$Ni$_6$) due to the increased distance of these atoms from the TM impurity. The spin densities of peripheral nickel atoms (MAl$_8$Ni$_6$) and that of interior atoms (MNi$_8$Al$_6$) are seen to be essentially identical, with net atomic moments ranging from 0.14 to $0.28\mu_B$ depending upon the TM impurity. For comparison, note that the Ni moment in AlNi$_8$Al$_6$ clusters is calculated as $0.07\mu_B$.

The eight equivalent Ni atoms in MNi$_8$ clusters (Table II) and in MNi$_8$Al$_6$ clusters (Table III) have similar charge populations, except for rearrangements of the $4s, p$ shell corresponding to formation of second-neighbor bonds. However, a reduction by a factor of ~ 3 in magnitude of spin density is noted for the larger clusters, suggesting an important role for second-neighbor Al atoms in determining response of the host to the magnetic impurity. There is now a clearer differentiation between moments of nonmagnetic AlNi$_8$Al$_6$ and NiNi$_8$Al$_6$ complexes and the iron and cobalt clusters. However, there is still no basis for discriminating between the "local-moment" Fe cluster and the Co system.

The Mössbauer isomer shift (IS) can provide further information about the impurity site. Although measurements are generally limited to ^{57}Fe in the $3d$ transition-metal series, there are a variety of suitable isotopes in the heavier transition metals. The IS is given[35] as a product of nuclear and electronic charge density differences between two different chemical environments A and B.

$$\Delta E_{IS} = \frac{2\pi}{3}Ze^2 \{\rho_A(0) - \rho_B(0)\} \{\langle R_e^2 \rangle - \langle R_g^2 \rangle\} \ ,$$

where ρ_A and ρ_B refer to the electronic densities at the nucleus in A and B, and $\langle R_e^2 \rangle$ and $\langle R_g^2 \rangle$ represent the mean-square radius of nuclear excited and ground states, respectively. This energy shift is usually expressed as the Doppler velocity of relative motion between the two environments

$$\delta_{AB} = \frac{c\Delta E_{IS}}{E_\gamma} = \alpha\Delta\rho(0) \ ,$$

where

$$\alpha = \frac{2c}{3E_\gamma}\pi Z e^2 \Delta \langle R^2 \rangle \ .$$

For ^{57}Fe the current value of the isomer shift calibration constant α is $\alpha = (-0.30 \pm 0.03) a_0^3$ mm sec^{-1}.[36]

Two measurements of the Mössbauer isomer shifts of ^{57}Fe impurities in β'-NiAl have been reported. In the first such study Frankel et al. measured the IS relative to ^{57}Co diffused in NiAl.[37] They obtained an IS of 0.36 mm/sec relative to sodium ferrocyanide for both NiAl and FeAl. They were not able to distinguish different shifts for Fe impurities on the two different lattice sites, but presumed that the ^{57}Co had diffused primarily onto the Ni lattice. The measurements of Wiley et al. indicate a small difference in the IS's of ^{57}Fe on the two lattices.[38] While measurements of Fe impurities in stoichiometric NiAl were not obtained for both lattice sites, the IS values of $Al_{50}Ni_{48}Fe_2$ and $(NiAl)_{98}Fe_2$ that they obtained can be compared. Since Al atoms do not substitute on the Ni lattice, it is believed that the $Al_{50}Ni_{48}Fe_2$ alloy favors Fe substitution on TM sites. In alloys like $(NiAl)_{98}Fe_2$, Fe should substitute on either site. The data of Ref. 38 indicate a small difference of (0.05 ± 0.02) mm/sec in the IS's of the two alloys, with the $Al_{50}Ni_{48}Fe_2$ alloy having the higher shift. If this is translated into site charge densities, then Fe substituted on the Ni lattice should have a charge density $\rho(0)$ lower by $\sim 0.17 e/a_0^3$ than if it were substituted on the Al lattice.

We have compared isomer shifts between the 9-atom clusters, $FeNi_8$ and $FeAl_8$ and between the 15-atom clusters, $FeNi_8Al_6$ and $FeAl_8Ni_6$. For all four clusters we obtain to five significant figures $\rho_{Fe}(0) = 12032 a_0^{-3}$. The variation in charge density between the clusters is thus in the sixth digit and about at the level of numerical noise in our calculations. This result is interesting in view of the somewhat different charge states indicated for Al site and Ni site substitution. Qualitatively our results are in good agreement with both experimental papers in that the charge density is very similar on both sites. Quantitatively, we obtain $\Delta\rho_{Fe}(0) = (-0.5 \pm 0.4) a_0^{-3}$ for the minimal clusters and $\Delta\rho_{Fe}(0) = (-0.1 \pm 0.2) a_0^{-3}$ for the larger clusters. These give isomer shifts of (0.15 ± 0.12) mm/sec and (0.03 ± 0.06) mm/sec, respectively. The results taken together indicate a very small shift of the same sign and approximate magnitude as that reported by Wiley et al.

The presence of unpaired spins induces a magnetic hyperfine field which can be probed at nuclear sites by NMR or Mössbauer γ-ray measurements. The NMR technique has been used very successfully to probe the induced spin density at varying distances from a TM impurity in systems like MnCu.[28] The magnetic hyperfine field at site $\vec{r}$ due to unpaired

spins is given by

$$H_s(\vec{r}) = -\frac{1}{3} 16\pi\mu_B \langle \sum_i s_i^z \delta(\vec{r}_i - \vec{r}) \rangle$$

$$= -\frac{1}{3} 8\pi\mu_B \sum_i \{n_i^\uparrow |\psi_i^\uparrow(\vec{r})|^2 - n_i^\downarrow |\psi_i^\downarrow(\vec{r})|^2\}$$

$$= 524.3 \text{ kG}/a_0^3 \, \rho_s(\vec{r}) \ ,$$

where the expectation value of the spin density ρ_s can be calculated as a sum of one-electron orbital contributions weighted by spin-dependent occupation numbers n_i^σ. The present iron impurity calculations indicate a nonzero hyperfine field at either substitutional site, $H_s \sim -30$ kG for $Fe_{Ni}(FeAl_8)$ and $H_s \sim +20$ kG for $Fe_{Al}(FeNi_8)$. The predicted difference in sign as well as in magnitude suggests that hyperfine field measurements could be used to make unambiguous determinations of the impurity site in these alloys, and would provide a basis for further tests of model theories.[28,39-41]

One such hyperfine field measurement has been reported by Frankel, Sellmyer, and Blum in which ^{57}Co was diffused into "near" stoichiometric NiAl.[37] Their measurements indicate a negligible hyperfine field at ^{57}Fe sites following radioactive ^{57}Co decay. However, uncertainty in alloy composition and limited spectral resolution of this work makes further studies desirable.

IV. CONCLUSIONS

We have used a self-consistent embedded-cluster model to study the properties of transition-metal impurities in the intermetallic compound β'-NiAl. It was necessary to first examine the bulk alloy from which an approximation of the crystal embedding field was derived. The calculated DOS of bulk β'-NiAl compared quite favorably with other theoretical calculations and also with experimental XPS and UPS data. Several different crystal potentials were evaluated in an attempt to approach the self-consistent result. We finally selected the configuration $Ni^{-0.12}Al^{+0.12}$ because it gave the most consistent results for all embedded clusters.

Transition-metal impurities found on Ni sites invariably show reduced moments compared to the free atom, with small polarizations on nearest-neighbor Al atoms. This result is at least consistent with experimental findings of no local-moment behavior for this site.

Transition-metal impurities found on Al sites generally show a sizable magnetic moment, with significant polarization of the nearest-neighbor Ni shell. The polarization of the Ni shell is found to be reduced in the larger MNi_8Al_6 clusters. No basis for distinguishing between transport properties of Fe- versus Co-doped alloys is found. We speculate that

coupling between impurity moment and host electrons is subject to time-dependent fluctuations which are not contained in static models. The present work does give a reasonable and consistent picture of the bonding and spin density for a static "paramagnetic" state of the system.

ACKNOWLEDGMENTS

*Permanent address: Dept. of Radiology, Univ. of Ill. at the Medical Center, Chicago, Ill. 60612.

[1]J. R. Willhite, L. B. Welsh, T. Yoshitomi, and J. O. Brittain, Solid State Commun. 13, 1907 (1973); J. R. Willhite, T. Yoshitomi, L. B. Welsh, and J. O. Brittain, in *Proceedings of the Nineteenth Conference on Magnetism and Magnetic Materials, Boston, 1973*, edited by C. D. Graham, Jr. and J. J. Rhyne, AIP Conf. Proc. No. 18 (AIP, New York, 1974), p. 272.

[2]M. B. Brodsky and J. O. Brittain, J. Appl. Phys. 40, 3615 (1969).

[3]M. Höhl, Z. Metallkd. 51, 85 (1960).

[4]Y. Yamaguchi, T. Aoki, and J. O. Brittain, J. Phys. Chem. Solids 31, 1325 (1970).

[5]G. R. Caskey, J. M. Franz, and D. J. Sellmyer, J. Phys. Chem. Solids 34, 1179 (1973).

[6]T. Yoshitomi, T. Ochiai, and J. O. Brittain, J. Phys. Chem. Solids 38, 533 (1977).

[7]Y. Ochiai and J. O. Brittain, Solid State Commun. 22, 443 (1977).

[8]Y. Yamaguchi and J. O. Brittain, Phys. Rev. Lett. 21, 1447 (1968).

[9]J. R. Willhite and J. O. Brittain, in *Proceedings of the 21st Conference on Magnetism and Magnetic Materials, Philadelphia, 1975*, edited by J. J. Becker, G. H. Lander, and J. J. Rhyne, AIP Conf. Proc. No. 29 (AIP, New York, 1976), p. 344.

[10]T. Yoshitomi, Y. Ochiai, and J. O. Brittain, Solid State Commun. 20, 741 (1976).

[11]J. C. Slater, *The Self-Consistent Field for Molecules and Solids* (McGraw-Hill, New York, 1974).

[12]J. C. Slater, Phys. Rev. 81, 385 (1951); 82, 538 (1951); R. Gaspar, Act. Phys. Acad. Sci. Hung. 3, 263 (1954); W. Kohn and L. J. Sham, Phys. Rev. 140, A1133 (1965).

[13]For example, see V. L. Moruzzi, A. R. Williams, and J. F. Janak, Phys. Rev. B 15, 2854 (1977); L. L. Boyer, D. A. Papaconstantopoulos, and B. M. Klein, Phys. Rev. B 15, 3685 (1977); T. J. Watson-Yang, B. N. Harmon, and A. J. Freeman, J. Magn. Magn. Mater. 2, 334 (1976).

[14]O. Gunnarsson, M. Jonson, and B. I. Lundqvist, Solid State Commun. 24, 765 (1977); L. Hedin and B. I. Lundqvist, J. Phys. C 4, 2064 (1971); P. Vashista and K. S. Singwi, Phys. Rev. B 6, 875 (1972).

[15]J. W. D. Connolly and K. H. Johnson, in *NBS 3rd Materials Research Symposium on Electronic Density of States*, edited by J. H. Bennett (NBS, Washington, 1971), p. 323; K. H. Johnson and J. W. D. Connolly, Int. J. Quantum Chem. 3, 813 (1970).

[16]V. L. Moruzzi, A. R. Williams, and J. F. Janak, Phys. Rev. B 10, 4856 (1974).

[17]A. Zunger and A. J. Freeman, Phys. Rev. B 16, 2901 (1977) and references therein.

[18]G. A. Baraff and M. Schlüter (unpublished).

[19]R. P. Messmer, C. W. Tucker, Jr., and K. H. Johnson, Chem. Phys. Lett. 36, 423 (1975).

[20]R. P. Messmer, S. K. Knudson, K. H. Johnson, J. B. Diamond, and C. Y. Yang, Phys. Rev. B 13, 1396 (1976).

[21]P. J. Jennings, G. S. Painter, and R. O. Jones, Surf. Sci. 60, 255 (1976).

[22]G. S. Painter, P. J. Jennings, and R. O. Jones, J. Phys. C 8, L199 (1975).

[23]T. Tanabe, H. Adachi, and S. Imoto, Jpn. J. Appl. Phys. 16, 375 (1977).

[24]T. Hori, H. Adachi, and S. Imoto, Trans. Jpn. Inst. Met. 18, 31 (1977).

[25]D. E. Ellis, G. A. Benesh, and E. Byrom, Phys. Rev. B 16, 3308 (1977).

[26]D. E. Ellis, G. A. Benesh, and E. Byrom, J. Appl. Phys. 49, 1543 (1978).

[27]F. W. Averill and D. E. Ellis, J. Chem. Phys. 59, 6412 (1973); A. Rosén, D. E. Ellis, H. Adachi, and F. W. Averill, J. Chem. Phys. 65, 3629 (1976).

[28]J. D. Cohen and C. P. Slichter, Phys. Rev. Lett. 40, 129 (1978) and references therein.

[29]R. S. Mulliken, J. Chem. Phys. 23, 1833 (1955); 23, 1841 (1955).

[30]R. W. G. Wyckoff, *Crystal Structures* (Interscience, New York, 1948).

[31]S. P. Kowalczyk, G. Apai, G. Kaindl, F. R. McFeely, L. Ley, and D. A. Shirley, Solid State Commun. 25, 847 (1978).

[32]P. O. Nilsson, Phys. Status Solidi 41, 317 (1970).

[33]J. Kondo, in *Solid State Physics*, edited by F. Seitz, D. Turnbull, and H. Ehrenreich (Academic, New York, 1969), Vol. 23, p. 184; A. J. Heeger, *ibid*, p. 284; M. Bailyn, Adv. Phys. 15, 179 (1966).

[34]See, for example: V. Korenman, J. L. Murray, and R. E. Prange, Phys. Rev. B 16, 4032 (1977); 16, 4048 (1977); 16, 4058 (1977).

[35]See, for example: N. N. Greenwood, and T. C. Gibb, *Mössbauer Spectroscopy* (Chapman and Hall, London, 1971).

[36]W. C. Nieuwpoort, D. Post, and P. Th. van Duijnen, Phys. Rev. B 17, 91 (1978).

[37]R. B. Frankel, D. J. Sellmyer, and N. A. Blum, Phys. Lett. A 33, 13 (1970).

[38]C. L. Wiley, L. B. Welsh, L. H. Schwartz, and J. O. Brittain, Phys. Lett. A 48, 474 (1974).

[39]P. Jena and D. J. W. Geldart, Phys. Rev. B 7, 439 (1973) and references therein.

[40]K. H. Johnson, D. D. Vvedensky, and R. P. Messmer, Phys. Rev. B 19, 1519 (1979).

[41]K. Aoi, H. Devling, and K. H. Bennemann, Phys. Rev. B 10, 1975 (1974).